

Identification of Abnormal System Noise Temperature Patterns in Deep Space Network Antennas Using Neural Network Trained Fuzzy Logic

Thomas Lu, Timothy Pham and Jason Liao
 Jet Propulsion Laboratory
 California Institute of Technology
 4800 Oak Grove Dr.
 Pasadena, CA 91109, USA

E-mails: Thomas.Lu@jpl.nasa.gov, Timothy.Pham@jpl.nasa.gov, Jason.Liao@jpl.nasa.gov

Abstract – This paper presents the development of a fuzzy logic function trained by an artificial neural network to classify the system noise temperature (SNT) of antennas in the NASA Deep Space Network (DSN). The SNT data were classified into normal, marginal, and abnormal classes. The irregular SNT pattern was further correlated with link margin and weather data. A reasonably good correlation is detected among high SNT, low link margin and the effect of bad weather; however we also saw some unexpected non-correlations which merit further study in the future.

Keywords - Deep Space Network; Neural network training; Fuzzy logic; Pattern identification; System noise temperature; Link margin.

I. INTRODUCTION

The communication between NASA space mission operations teams and their respective spacecrafts in outer space is accomplished via the Deep Space Network (DSN). To ensure proper operations in returning telemetry data to mission operations, sending commands to spacecraft and providing radiometric data for navigation purposes, the DSN equipment generates a large set of self-monitor data. These include key metrics of system performance such as antenna pointing, operating system noise temperature, receiver and decoder lock indications, received telemetry symbol signal-to-noise ratio, telemetry frame quality, etc. These data statistics are generated periodically, in the order of a few seconds, throughout the spacecraft tracking passes. With roughly 1500 tracking passes a month, there is a lot of monitored data to be evaluated.

The DSN recently developed the capability to automatically quantify key metrics through a set of automated performance dashboards, as reported in [1]. These dashboards enable a quick detection of passes with anomalous performance – compared to those that are nominal. One of the tools used to classify the performance of the passes is the fuzzy logic function described in this

paper. This function is trained by an artificial neural network to classify the system noise temperature (SNT).

The SNT reflects the amount of noise that existed in the communications system. Given that the signal comes from a far-away spacecraft at planetary distance, the received power is very weak. The ability to detect the signal is affected by the system noise temperature; the lower the noise, the better chance the system can detect the signal. Thus, there is a strong interest in monitoring and classifying the SNT.

The next section describes key features that are used to distinguish various classes of SNT profiles. Structure of the neural network model employed in the data classification and the recognition training process are presented in Section III. Section IV provides the results of the SNT classification, in terms of the impact to the link conditions (e.g., good, bad, marginal). Further correlation between SNT categories and the link margin of the communications channel with spacecraft is shown in Section V. Section VI further extends the correlation between the SNT and weather – one of the key factors impacting the link margin. The final section summarizes and discusses future direction of this effort.

II. SYSTEM NOISE TEMPERATURE FEATURES

Figure 1 shows a typical sample of SNT measurement for a given pass, in this case with Voyager spacecraft on day-of-year (DOY) 320/2007. Within the figure are plots of predicted SNT (labeled as 810-5, per reference of a JPL-internal document number that reflects such a model), observed SNT, and antenna pointing elevation. The antenna elevation is one of the parameters that affect the SNT. At low elevation, there are more atmospheric layers in the signal path; resulting in a higher noise temperature. The effect of elevation is built into the modeling of the predicted SNT. In this particular pass, the measured SNTs (Blue line) closely follow the predicted curve (Gray line, 810-5).

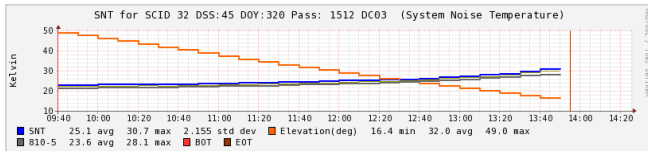
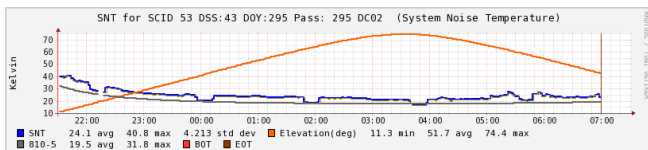
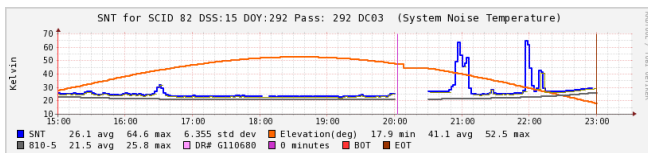


Figure 1: SNT observed and predicted measurement, DOY 320/2007.

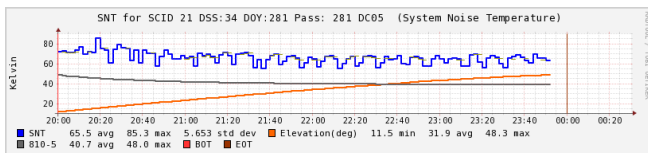
However, sometimes the measured SNT curve would deviate from the predicted performance slightly, as shown in Figure 2(a). At times, there could be very dramatic deviation, as shown in Figures 2(b) and (c). Some of these are known, such as the variation in Figure 2(b) was likely caused by weather conditions. Other variations such as the periodic structure in Figure 2(c) are not fully understood. Our goal is to use the pattern recognition tool described in this paper to find those irregular patterns and then study the causes in details.



(a)



(b)



(c)

Figure 2: Irregular SNT measurement data from various passes.

A simple threshold method may not be able to sufficiently characterize the SNT data since there could be sudden perturbations as shown in the right side of Figure 2(b). The SNT measurement follows the predicted model nicely between 15:00-20:00 GMT, but there are two big peaks around 21:00 and 22:00 GMT, likely caused by bad weather. A simple threshold or mean/standard-deviation method could have missed this event. A more intelligent signal processing method, such as neural network, may be able to detect the abnormal patterns of SNT.

In order to capture various irregular patterns of SNT data, we have designed a set of features of the SNT curves: mean values, standard deviations, peak numbers, peak-to-valley variations, and slope of the peaks. The SNT data for various passes are processed to extract the SNT curve feature vectors; each pass is represented by a feature vector. Each feature vector consists of six elements:

1) Average SNT Difference (from model):

$$\Delta SNT_{ave} = \frac{\sum (SNT_m - SNT_p)}{n} \quad (1)$$

where SNT_m is the measured SNT sequence of pass m with length n. SNT_p is the corresponding predicted values for that m pass.

2) Standard Deviation:

$$STD = \sqrt{\frac{\sum ((SNT_m - SNT_p) - \Delta SNT_{ave})^2}{n}} \quad (2)$$

3) Estimated 1-sigma higher bound of variation:

$$\Delta SNT_h = \Delta SNT_{ave} + STD; \quad (3)$$

4) Estimated 1-sigma lower bound of variation:

$$\Delta SNT_l = \Delta SNT_{ave} - STD; \quad (4)$$

5) SNT Peak Number:

$$K = \text{Number of peak and valley pairs}; \quad (5)$$

where Peak-to-Valley Difference $> STD$;

6) SNT Peak Slope:

$$\text{Slope} = \frac{\text{Max}(Peak_k - Valley_k)}{K}; \quad (6)$$

We need to define the criteria for the SNT irregularities. Since there is no known set rule, we choose the following definition based on observation and experience.

- 1) Averaged SNT is more than 10 K above the performance model, i.e., Averaged SNT Difference, $\Delta SNT_{ave} > 10K$;
- 2) Averaged SNT is more than 10 K below the performance model, i.e., Averaged SNT Difference, $\Delta SNT_{ave} < -10K$;
- 3) Peak to valley variation $> 20 K$;
- 4) Slope $> 5 K/\text{minute}$ or Slope $< -5K/\text{minute}$.

Since the criteria are not simple Boolean operations and that there may be a need for adding non-threshold criteria in later analysis, we were concerned that a simple threshold approach may not be suitable for classifying the SNT patterns. Therefore we decided to design a Fuzzy logic to classify the SNT patterns. A neural network is then used to train the fuzzy logic.

III. NEURAL NETWORK TRAINING

An artificial neural network is an adaptive computational model inspired by the study of biological neural networks [2]. It mimics human biological neural functions that learn by example. The neural net used in this system is a feed-forward back-propagation model, as illustrated in Figure 3. It is composed of separate layers of connected units called neurons. Every neuron of one layer is connected to every neuron of the next layer and each connection has an assigned weight value w . The output of a neuron y in the $(k+1)$ th layer is calculated by a weighted sum of the inputs, x , in the k th layer into that neuron [3]:

$$y_j^{k+1} = f\left(\sum_{i=1}^N w_{ij}^k x_i^k + b_j^k\right) \quad (7)$$

where f is a Sigmoid transfer function which maps the input-output relationship into a range [0, 1].

The feature vector serves as the initial input into the neurons of the first hidden layer. The output of neurons from one layer then feeds into the neurons of the next layer until the output layer returns a confidence value between [0, 1]. This architecture is known as feed-forward neural net.

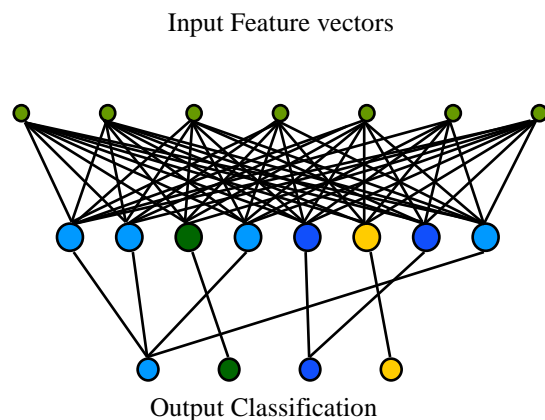


Figure 3: Multi-layer feed-forward neural network architecture.

The neural network classifies an input data to an output class, giving a confidence value between the probability from 0 – 100%. Thus a Fuzzy logic is formed between the input data and the output classes [4].

Figure 4 illustrates the neural network training process. A person with domain knowledge first picks a set of training SNT data. The expert must assign the SNT data (training inputs) into correct classes (target outputs). The feature vector is extracted from a set of SNT data, presented to the input neurons of the neural network; the neural network feed-forwards the signal and makes an attempt to classify the input to an output class; the output result is compared to the target output; the output error is

used to back-propagate through the network to tune the weights. The learning process is repeated many times until the output error of the neural network is less than a set value [5-7].

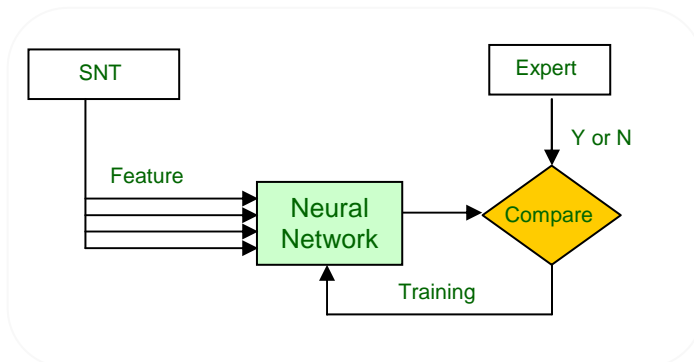


Figure 4: Illustration of neural network training process.

We used a set of SNT data from DOY 001-065 in 2007 as the training and testing data. There were a total of 1950 SNT data in the test set. Among them, there were 1329 (68.2%) valid SNT data to classify. The SNT data are classified into six categories based on observation of the patterns, as shown in Table I. Category 1 represents large SNT deviation with large peaks and slopes; Category 2 has large but smooth positive deviations; Category 3 has small deviations and small perturbations; Category 4 follows the predicted SNT consistently; Category 5 has small and smooth deviations; Category 6 has large and smooth negative deviations.

TABLE I. DEFINITION OF SNT CATEGORIES

SNT Category	Features
1	$\Delta SNT_{ave} > 10K$ or $\Delta SNT_{ave} < -10K$ or Slope $> 5K/min$ or Peak No > 5
2	$\Delta SNT_{ave} > 10K$, Slope $< 5K/min$, Peak No < 5
3	$\Delta SNT_{ave} < +/-10K$, STD $\leq 3K$, Slope $< 5K/min$, Peak No < 5
4	$\Delta SNT_{ave} \leq +/-5K$, STD $\leq 3K$, Slope $< 5K/min$, Peak No < 0
5	$\Delta SNT_{ave} \leq +/- 5K$, STD $\leq 3K$, ΔSNT_h and $\Delta SNT_l < +/-5K$, Slope $< 5K/min$, Peak No < 2
6	$\Delta SNT_{ave} < -10K$, STD $\leq 3K$, Slope $< 5K/min$, Peak No < 5

To form the training data, we randomly picked 39 samples for Category 1; 33 samples for Category 2; 61 samples for Category 3; 69 samples for Category 4; 35 samples for Category 5; and 26 samples for Category 6. The training samples are hand picked to represent varieties of feature differences in all six categories. We constructed a three-layer feed-forward neural network, each layer consists of six neurons: six input neurons for the six input

features; six output neurons for the six categories, and six hidden layer neurons are chosen to accommodate non-linear boundaries. The training data is fed into the neural net in the Matlab program. The neural net converged rather quickly; it took less than two minutes on a Windows-based computer with Intel dual-core running at 2GHz. After the training, the tool is ready for use to classify the SNT data.

IV. CLASSIFICATION OF SNT DATA

Table II shows the initial classification of the SNT data. The features were extracted based on eqs. 1-6. The six feature elements were fed into the neural network. When one or more of the six output neurons exceeded a preset threshold (nominally, 50%), the neural net would classify the input SNT as belonging to the output categories. An input could be classified in more than one category, as long as all possible likelihoods were detected. This is reflected in Table II where there is an overlap in the percentage of each category, relative to the input samples.

It is often difficult to have a clear cut set of the boundaries between categories; for example, it is hard to define a priori of the number of peaks or the peak slope value in each category. A Boolean classification approach would require such parameters be defined ahead of time. With neural net approach, it is not necessary to do so. We can pick the training samples that we believe are representative to each category, use them to train the fuzzy logic, and let the neural net feedback do the detection.

TABLE II. INITIAL CLASSIFICATION OF SNT DATA

SNT Category	No. of SNT Data	Percentage
1	170	12.9%
2	1158	87.1%
3	1030	77.5%
4	1017	76.5%
5	1004	75.5%
6	851	64.0%

In Table III, we further reduce the classes into three major classes: "Good", "Marginal" and "Bad". The neural network is constructed as six inputs, six hidden, and three output neurons. In this case, for each input data, we only pick the highest output neuron that is greater than 50% as the category. For the dates between DOY 1-65/2007, the neural network classified 67.7% of data as "good", 19.9% "Marginal", and 12.3% "Bad" data. This is a qualitative classification. Not all "Bad" SNT data result in severely impacted link performance. Further investigation is

warranted to further study the behavior of the SNT pattern related to the DSN data quality.

The neural net/fuzzy logic provides an effective tool for the SNT quality assessment. Figure 5 shows the performance of various antennas (designated as DSS) based on the SNT classification. Good SNT varies from an average of 43% (DSS-63) to 96% (DSS-14).

TABLE III. USING FUZZY LOGIC TO CLASSIFY SNT DATA INTO THREE CATEGORIES

Category	Classification	Feature Extraction	No. of SNT Data	Percentage
1	Good: SNT matches performance model	$\Delta SNT_{ave} < +/- 5K$, ΔSNT_h and $\Delta SNT_l < +/- 5K$, Slope $\leq 5K/min$, Peak No ≤ 2	853	67.7%
2	Marginal: SNT has minor deviation from performance model	$\Delta SNT_{ave} \leq +/- 10K$, ΔSNT_h and $\Delta SNT_l \leq +/- 10$, Slope $\leq 5K/min$, Peak No ≤ 5	251	19.9%
3	Bad: SNT has major deviation from performance model	$\Delta SNT_{ave} > +/- 10$, ΔSNT_h and $\Delta SNT_l > +/- 10$, Slope $> 5K/min$, Peak No > 5	155	12.3%

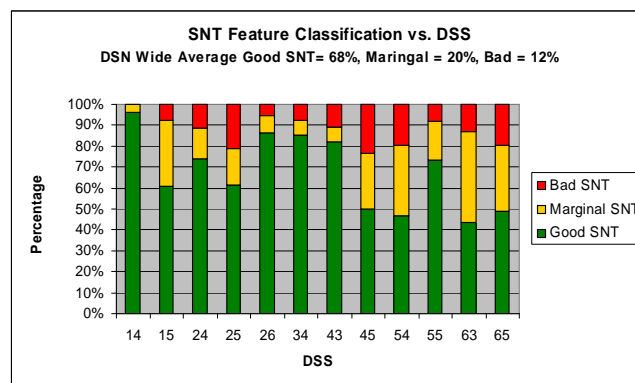


Figure 5: Classification of SNT data for various DSN antennas (DSS), DOY 1 – 65, 2007.

V. CORRELATION BETWEEN SNT AND LINK MARGIN

The Link Margin (LM) is one of the major indicators of the data communication quality. It is defined as the difference between the received symbol SNR (signal-to-noise ratio) and the decoder threshold required for

successfully decoded data. A positive link margin implies a good communications channel condition; the higher the margin, the less likely the link encounters data corruption. A negative margin, on the other hand, indicates likelihood with data demodulation and decoding; thus, would negatively affect the data return to missions. There is an inverse relationship between the SNT and link margin. An increase in noise temperature would reduce the received signal-to-noise ratio (SNR) and subsequent link margin, and vice versa. The correlation coefficient is defined as:

$$CorrCoef = \frac{\sum \Delta SNT_{ave}(i) LM(j)}{\sqrt{\sum \Delta SNT_{ave}(i)^2 \sum LM(j)^2}} \quad (8)$$

where LM is the average link margin of a given pass and where both the ΔSNT_{ave} and LM data are normalized to be within (-1, 1).

The correlation coefficient shows the relationship between the SNT and LM:

- If the ΔSNT and LM are positively correlated, then $Corr\ Coef > 0$;
- If the ΔSNT and LM are negatively correlated, then $Corr\ Coef < 0$;
- If the SNT and LM are uncorrelated, then $Corr\ Coef = 0$;

Figure 6 shows the ΔSNT -LM correlation at DSS-45 antenna for Voyager (VGR2) passes. From the graph, we can see the ΔSNT and LM data from VGR2 data are strongly negatively correlated, with $Corr\ Coef = -0.64$. It means that if the average SNT difference from the performance model increases, it will cause the link margin to drop, as expected.

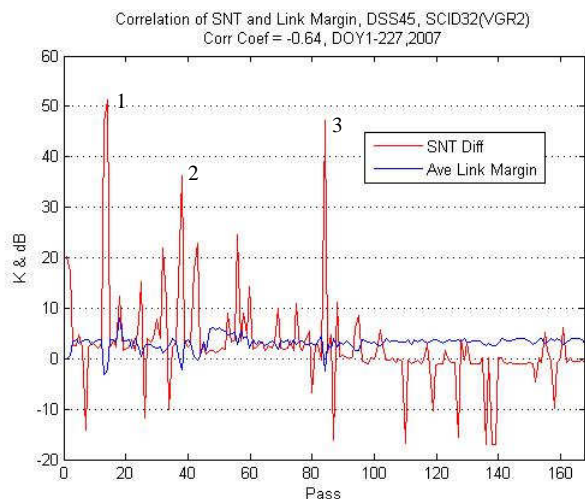


Figure 6: Correlation between SNT and Link Margin (LM) of VGR2 on DSS45 shows strong negative correlation (Corr Coef = -0.64).

We further analyze the relationship between the ΔSNT and LM in the three spikes (#1, #2, and #3) in Figure 6

In Figure 7, we can see an increased slope of the SNT between 7:47 and 9:08 GMT caused a drop in the link margin. In both Figures 8 and 9 for VGR2 passes on DOY 54 and DOY 117, we also see an increased slope of the SNT matched with a drop in link margin.

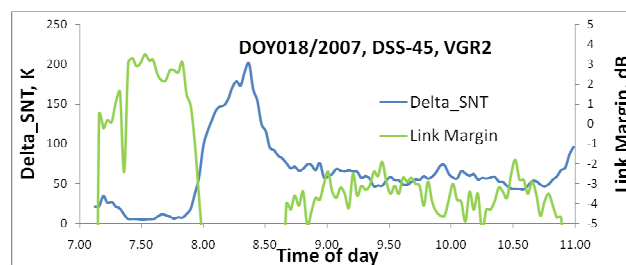


Figure 7: Negative correlation between SNT and Link Margin seen in VGR2 data on DOY18/2007 pass at DSS45.

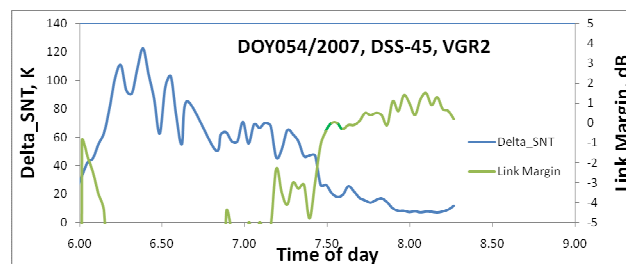


Figure 8: Negative correlation between SNT and Link Margin seen in VGR2 data on DOY 54/2007 pass at DSS45.

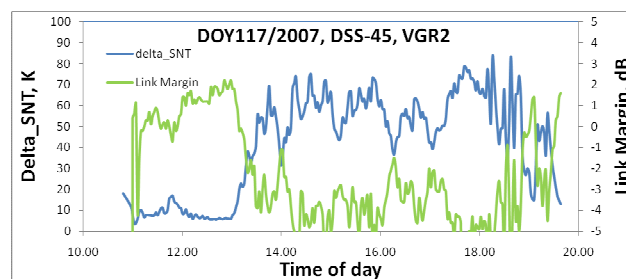


Figure 9: Negative correlation between SNT and Link Margin seen in VGR2 data on DOY 117/2007 pass at DSS45.

However, not all data have expressed a strong negative correlation between SNT and LM. We have observed that some other spacecraft data are either weakly negatively correlated ($Corr\ Coef = -0.2 - -0.3$), or uncorrelated ($Corr\ Coef = -0.2 - +0.2$). More validation effort is needed to understand these instances.

VI. CORRELATION OF SNT CLASSIFICATION WITH WEATHER

In this section, we extend the correlation to include the weather effect. Atmospheric effects in the line of sight between the ground tracking antenna and spacecraft are reflected in the observed system noise temperature measurements. Increased precipitation from rain and increased humidity would cause a higher SNT. Figure 10(a) shows the weather data during the pass. The cumulative precipitation for the day, reflecting the rain, is seen occurring at 15:00 – 18:00 GMT. The SNT starts to depart from a modeled curve and steady increases over the same period, per Figure 10(b). The received symbol signal to noise ratio, in Figure 10(c), drops as much as six (6) dB over the same period.

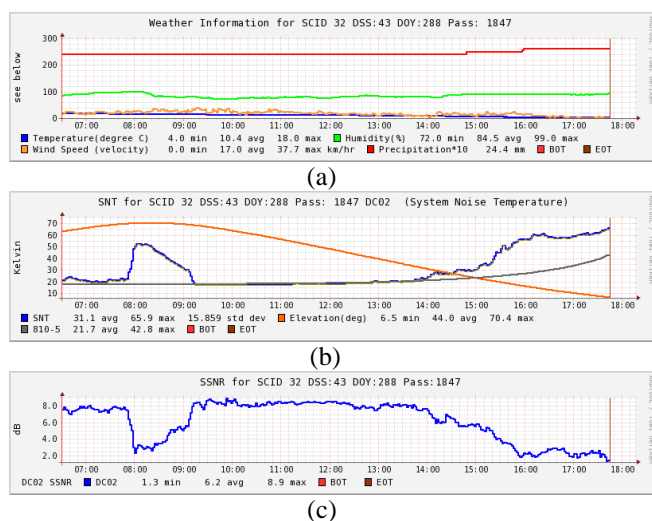


Figure 10: Correlation between (a) high SNT peaks, (b) low Link Margin, and (c) bad weather.

There is a general positive correlation among the changes in SNT, link margin and weather precipitation in this case. Note that there was similar increased SNT and decreased symbol SNR near 8:00 GMT, but surprisingly there was no indication of rain from the cumulative precipitation measurements. This is an example of possible inconsistency among the observables. Such obstacle would be hard to overcome for a detection scheme using Boolean logic. The neural network approach, given proper training data, may offer a way to overcome these difficulties.

VII. CONCLUSIONS AND FUTURE DIRECTION

We have presented the development of a neural network trained Fuzzy logic for system noise temperature classification. With the inherent advantage of neural network training using examples without setting concrete

rules, we have trained the neural network to evaluate the characteristics of measured SNT and to classify its impact to the communications link. We have observed, as expected, some correlations between “Bad” SNT category and low link margin conditions, which would affect the mission data return. In the future, adding link margin information to the training of the SNT classification should help to improve the results. Further analysis of other observed signatures of SNT deviation beyond the standard six categories discussed in this paper would further the understanding on the operating behavior and performance of DSN antennas; thus, pointing the way to possible improvement. Certainly, the potential application of this pattern recognition algorithm to other areas of DSN performance analysis should be considered.

ACKNOWLEDGMENTS

This research was carried out at the Jet Propulsion Laboratory, California Institute of Technology under a contract with the National Aeronautics and Space Administration (NASA).

REFERENCES

- [1] Pham, T. and Liao, J., “DSN Performance Dashboards”, SpaceOps 2008, Heidelberg, May 2008.
- [2] Jain, A. K., Mao, J., and Mohiuddin, K. M., “Artificial Neural Networks: A Tutorial,” *Computer*, vol. 29, no. 3, 1996, pp. 31-44.
- [3] Hagan, H. T., Demuth, H. B., and Beale, M.H., *Neural Network Design*, Martin Hagan, 2002.
- [4] Yager, R. et al. ed., *Fuzzy Sets and Applications: Selected Papers by L.A. Zadeh*, John Wiley, New York, 1987.
- [5] Ye, D., Edens, W., Lu, T., and Chao, T., “Neural Network target identification system for false alarm reduction,” *Optical Pattern Recognition XX*, Proceedings of the SPIE, Volume 7340, 2009.
- [6] Lu, T. and Mintzer, D., “Hybrid neural networks for nonlinear pattern recognition,” *Optical Pattern Recognition*, ed. by F. T. S. Yu and S. Jutamulia, Cambridge University Press, 1998.
- [7] Lu, T. and Lerner, J., “Spectroscopy and hybrid neural network analysis,” *Proceedings of the IEEE*, Volume 84, Issue 6, 1996, pp 895 – 905.